

## Temperature distribution behaviors of GFRP honeycomb hollow section sandwich panels

B. Kong<sup>a</sup>, C.S. Cai<sup>\*</sup> and F. Pan<sup>a</sup>

Department of Civil and Environmental Engineering, Louisiana State University, 3418 Patrick Taylor Hall,  
Nicholson Extension Dr., Baton Rouge, 70803 LA, USA

(Received August 23, 2012, Revised August 8, 2013, Accepted August 16, 2013)

**Abstract.** The fiber-reinforced polymer (FRP) composite panel, with the benefits of light weight, high strength, good corrosion resistance, and long-term durability, has been considered as one of the prosperous alternatives for structural retrofits and replacements. Although with these advantages, a further application of FRPs in bridge engineering may be restricted, and that is partly due to some unsatisfied thermal performance observed in recent studies. In this regard, Kansas Department of Transportation (DOT) conducted a field monitoring program on a bridge with glass FRP (GFRP) honeycomb hollow section sandwich panels. The temperatures of the panel surfaces and ambient air were measured from December 2002 to July 2004. In this paper, the temperature distributing behaviors of the panels are firstly demonstrated and discussed based on the field measurements. Then, a numerical modeling procedure of temperature fields is developed and verified. This model is capable of predicting the temperature distributions with the local environmental conditions and material's thermal properties. Finally, a parametric study is employed to examine the sensitivities of several temperature influencing factors, including the hollow section configurations, environmental conditions, and material properties.

**Keywords:** FRP panel; thermal effect; bridge; temperature change; modeling

---

### 1. Introduction

Composite materials have been developed and applied to the military aircrafts and aerospace equipment since World War II. In bridge engineering, the original design and construction of structures with composite materials were also mainly intended for military services, such as for quick bridge erections and rapid military deployments. During the past several decades, with the decrease of FRP's costs and development of manufacturing techniques, composite materials have begun to be applied in the civilian areas. Among all the applications, the FRP composite panels, with the advantages of high strength, light weight, quick installation time, good corrosion resistance, and long-term durability, are considered as one of the prosperous alternatives for structural retrofits and replacements. A state-of-the-art survey and the present and future utilizations of FRP composites in civil engineering have been well reported (Foster *et al.* 2000, Hollaway 2010, Bakis *et al.* 2002).

---

\*Corresponding author, Edwin B. and Norma S. McNeil Distinguished Professor, E-mail: [cscail@lsu.edu](mailto:cscail@lsu.edu)

<sup>a</sup>Research Assistant

Though with many benefits, the FRPs have not been widely applied in bridge engineering nowadays. The reasons are partly due to the lack of knowledge on the responses of such bridges under their distinctive material and structural properties. Different from traditional concrete and steel materials, composite materials are generally heterogeneous and non-isotropic. Their properties are largely determined by the component types, volume percentages, layout orientations, manufacturing methods, and bonding materials. This special characteristic can help engineers to design composite structures for specific demands, such as high-strength laminates for structure rehabilitations or light-weight panels for slab replacements. However, these designed structures may show negative performance in some aspects. The thermal response of FRP panels discussed in this study is one of the recent concerns in bridge engineering.

For the thermal properties of FRPs, such as the coefficients of expansion and conduction, they can be significantly different from those of the traditional steel and concrete materials, and can also be distinctive in the directions parallel and perpendicular to the fibers (Tipirneni 2008). Thus, when applied to bridges or assembled with other components, the FRP structures may produce complicated thermal responses and violate the current strength and service limits in design. For example, as indicated by the Federal Highway Administration (FHWA) (<http://www.fhwa.dot.gov/bridge/frp/deckprac.cfm> 2011), FRPs may be rapidly heated when exposed to the direct sunlight, and that can lead to large temperature differences between the top and bottom surfaces of the decks. These large thermal gradients, on one hand, can induce hogging and sagging actions affecting the performance of bearings, anchorage details, and panel movements; on the other hand, the induced thermal stresses can cause wearing surface cracks, delamination, and debonding failures.

While the study on the thermal behaviors is no longer a new topic for traditional concrete and steel bridges, similar studies are not adequate for FRP composite bridges. Oghumu (2005) developed a full 3D finite element model to investigate the local stresses and delamination problems at the interfaces between the facial and core of a GFRP panel under uniform and linear temperature variations; Laosiriphong *et al.* (2006) studied the thermal performance of a FRP deck through lab tests and correlated the responses with theoretical results; Liu *et al.* (2008) discussed the deflections of the first No-Name Creek FRP composite bridge built in US under temperature loadings; and Reising *et al.* (2004) compared the behaviors of four different FRP composite panels under the same environmental conditions and investigated the temperature induced delamination failures, large thermal gradients, and panel movements. Besides these studies, however, the experimental tests or numerical studies, are barely, if any, being conducted to study the temperature distribution behaviors for those recently applied FRP panels in bridge engineering. An accurate prediction of the temperature distributing pattern is always significantly important to understand the thermal performance of bridges; and it is also crucial in the further analysis of other deformations and forces induced by the temperature variations.

In response to this need, a field monitoring program was conducted by Kansas Department of Transportation (DOT) on a GFRP honeycomb hollow section sandwich panel bridge, located at Crawford County, KS. The instrumentations were mounted on the top and bottom panel surfaces, and the temperatures of the panels and ambient air were recorded every two hours from December 2002 to July 2004. This paper firstly demonstrates and discusses the temperature variation behaviors at the panel surfaces based on the field measurements. Then, a transient-state thermal field analysis, using the commercial software ANSYS 11.0, is conducted to examine the temperature distribution behaviors along the panel depths. Finally, a parametric study is employed to investigate the sensitivities of several influencing factors on the temperature distributions,

including the section hollowness, material thermal properties, and environmental conditions. It should be noted that the scope of this study is specific for, but not limited to, the temperature behaviors of GFRP panels. The observations obtained here can provide a meaningful reference to understand the temperature behaviors of other FRP panels. The proposed modeling method will be suited for the study of new composite panels when they are available in the future market.

## 2. Heat transfer mechanism

The temperature modeling methodology for traditional concrete and steel bridges has been well documented (Priestley 1978, Elbadry and Ghali 1983, Moorty and Roeder *et al.* 1992, Mirambell and Aguado 1990). Some of the information is briefly summarized in this section for the convenience of discussions. More importantly, the assumptions and parameters, which are adopted in the panels' temperature model discussed later, are explained in details corresponding to the heat transfer mechanisms.

### 2.1 Heat transfer equation

The transient-state temperature distribution behavior within a bridge is governed by a partial differential heat transfer equation as

$$\rho c \frac{\partial T}{\partial t} = k_x \frac{\partial^2 T}{\partial x^2} + k_y \frac{\partial^2 T}{\partial y^2} + k_z \frac{\partial^2 T}{\partial z^2} \quad (1)$$

where,  $\rho$  = material density;  $c$  = material specific heat;  $T$  = bridge temperature;  $t$  = time;  $k_x$ ,  $k_y$ , and  $k_z$  = material thermal conduction coefficients in the directions of  $x$ ,  $y$ , and  $z$ , respectively; and  $x$ ,  $y$ , and  $z$  = coordinates in three directions. For a bridge under natural environmental conditions, the 3D temperature transferring behavior, expressed as Eq. (1), can often be simplified into a 2D one, where the temperatures along the longitudinal direction of the bridge are observed too small to be neglected. In addition, the temperature differences in the transverse direction, noteworthy for those bridges with large thermal inertia, such as box girder bridges, can also be reasonably ignored for GFRP panels in this study due to their small thermal inertia. As a result, the 3D thermal behavior is finally simplified into a 1D one in the following temperature model.

### 2.2 Boundary condition

Many factors can affect the temperature field of a bridge under natural environmental conditions, e.g., solar, ambient air, wind, rain, snow, etc. Modeling all of these factors is infeasible and unnecessary; since most of them often make negligible or short-term effects thus not considered in design. Therefore, three major mechanisms are considered in this study, including (1) the conduction behavior through the bridge body due to temperature differences governed by the Fourier's equation, (2) the convection behavior between the structure surfaces and adjacent ambient air described by the Newton's law of cooling, and (3) the radiation behavior through emitting and receiving the electromagnetic energy defined by the Stefan-Boltzmann Law. Thus, the equilibrium equation for the solar radiation, surface convection, surface radiation, and body conduction, respectively, can be expressed as

$$\eta I_n - h_c(T_s - T_a) - \varepsilon\sigma(K_s^4 - K_a^4) + k_n \frac{\partial T}{\partial n} = 0 \quad (2)$$

where  $\eta$  = material solar absorptivity coefficient;  $I_n$  = solar input flux on the bridge surfaces;  $h_c$  = convection coefficient between the bridge surfaces and adjacent ambient air;  $T_s$  = bridge surface temperature;  $T_a$  = ambient air temperature;  $\varepsilon$  = material emissivity coefficient;  $\sigma$  = Stefan-Boltzmann constant;  $K_s$  = absolute bridge surface temperature;  $K_a$  = absolute ambient air temperature; and  $k_n$  = material thermal conduction coefficient.

### 2.3 Environmental and thermal parameters

Considering the boundary conditions for Eq. (2), three categories of parameters are required as input in the model, including environmental conditions (i.e., solar flux and ambient air temperature), material thermal properties (i.e., coefficients of thermal conductivity, solar absorptivity, and emissivity), and coefficients of thermal convection (related to the wind speed and material surface roughness). In the numerical model, the environmental condition can be obtained from the local weather stations or field measurements. If both of them are not available, they could be approximately predicted through numerical simulations. For example, the hourly-varying ambient air temperatures are predicted by interpolating a sinusoidal curve using the maximum and minimum daily ambient air temperatures. The solar input flux is calculated considering the solar input energy, time of the year, solar incident angles, effects of the atmosphere, environmental clearness conditions, etc. (Dilger *et al.* 1983, Duffie and Beckman 1980).

For the material properties and thermal parameters of FRPs, they are mostly case-dependent and largely determined by the constituents. They cannot be directly obtained from the current design manuals as those of traditional concrete and steel materials. Thus, an analytical method, which is based on the knowledge of micro-macro mechanics, is adopted in this study for the predictions of material properties. Generally speaking, the FRP material is in a laminated configuration composed of a few layers, where each layer is called a lamina. The micro-mechanical analysis is to develop the properties for each lamina, and the laminate properties are obtained by assembling the properties of each lamina through the macro-mechanical analysis thereafter. This simplified method is commonly utilized in the routine design of FRP materials. It enables to provide reasonable results for uniformly arranged materials, e.g., unidirectional fiber components (UNC), since they have dominant properties in the direction parallel and perpendicular to the fibers. For some other cases with randomly oriented fibers, however, the analytical results may produce some errors but are still within the tolerance for engineering applications.

## 3. Field monitoring study

### 3.1 Project description

The bridge studied here originally had an asphalt-on-steel deck supported by fourteen W21×68 I-beam stringers. The bridge deck was later replaced by five GFRP honeycomb hollow section sandwich panels laying perpendicular to the girders, as shown in Fig. 1. Kansas DOT measured the temperatures of the panel surfaces and ambient air every two hours from December 2002 to July 2004 (Meggers 2006).



Fig. 1 GFRP honeycomb hollow section sandwich panel bridge, KS

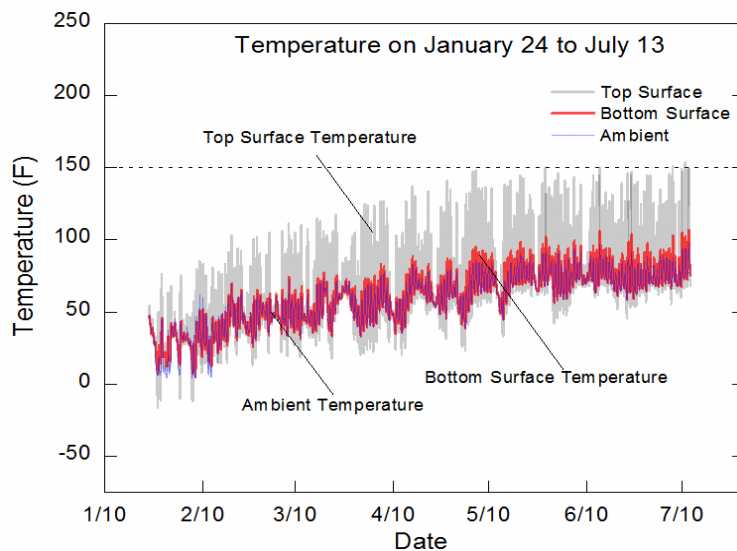


Fig. 2 Measured temperatures from January 24 to July 13, 2004

### 3.2 Monitoring results

The seasonal-varying temperatures (i.e., January 24 to July 13 in 2004) and the detailed hourly-varying temperatures during the warmest week (i.e., June 21 to June 27) and the coldest week (i.e., February 7 to February 14), respectively, are selected throughout the subsequent discussions. Based on these observations, some of the uncertainties on the temperature distribution behaviors of GFRP panels are tentatively clarified, including (1) the variation patterns at the panel surfaces, (2) the differences between the behaviors of GFRP panels and that of the concrete slabs as specified in the AASHTO LRFD (2007), and (3) the effects of the environmental conditions and material parameters. In addition, the wind speed, another important influencing factor, is obtained from the nearest weather station, Konza Prairie Biological Station, which is located at Manhattan, KS, with

the latitude and longitude of 39.1027N, 96.6098W (<http://www.ncdc.noaa.gov> 2012). Therefore, some of the findings are summarized as follows:

(1) Fig. 2 shows the temperature variations at the panel surfaces from January 24 to July 13 in 2004. For the temperatures at the top surfaces, they are significantly fluctuated and evidently higher than that of the ambient air. This phenomenon should be both related to the radiation behavior from the solar and the large energy absorption ability of the panels. While for the temperatures at the bottom surfaces, they are almost consistent with that of the ambient air, and that should be primarily affected by the air convection. In addition, the highly-varying heat energy at the top surfaces influences the temperatures at the bottom to a limited extent. In this sense, it may indicate that the current GFRP panels have low thermal conduction abilities; and that, in turn, may be attributed to the small conduction coefficients of the FRP materials or the hollow configurations of the panels.

The night sky radiation behaviors, when the temperatures of the panels are lower than that of the ambient air, are also observed in Fig. 2. Specifically, during the night, when the panel surfaces face the night sky, the heat is lost to the sky by radiation and, simultaneously, gained from the surrounding air by convection. If the surface is a good radiation emitter or the convection behavior is weak, it tends to radiate more heat than it gains. As a result, the temperatures at surfaces can drop below to that of the ambient air. The night sky radiation behavior often induces a negative thermal gradient distribution with a larger surface temperature at the bottom than that at the top. In the present case, the frequent occurrence of the night sky radiation behaviors observed during the monitoring period may imply that the negative thermal gradients are common for GFRP panel bridges.

(2) Fig. 3 and Fig. 4 show the hourly-varying temperatures during the warmest and coldest week, respectively. Sinusoidal variation trends can be approximately observed, which verifies the method introduced above that the temperatures of the bridges can be predicted by that of the ambient air. In addition, the temperatures at top surfaces are generally varying in the same pace as that at the bottom. In this sense, the temperature lagging effects can be reasonably ignored for this GFRP panel and the small thermal inertia assumption made above is justified.

For concrete slabs, the AASHTO LRFD (2007) specifies a difference of 25°C (46°F) positive gradient through the slab depths; and the positive gradient is multiplied by a coefficient to obtain the negative gradient, i.e., -0.3 and -0.2 for the plain concrete decks and asphalt overlaid decks, respectively. According to the measurements during the warmest and coldest week in this study, the maximum temperature differences between the top and bottom surfaces are 28°C (51°F) and 7°C (12°F), respectively. In this sense, the temperature differences of the current GFRP panels, though not the worst case yet, are already extending the range as specified for concrete slabs 25°C (46°F). Therefore, the available temperature design guidelines in the AASHTO LRFD (2007) may no longer be effective and safe for FRP panel bridges.

(3) Fig. 5 shows the measured environmental conditions at the bridge site and weather station. Although they are not exactly at the same location, the environments at the weather station can approximately represent that at the bridge site since the measured air temperature variations are almost similar in both places. Based on the measurements, the wind speeds at the weather station are generally lower than 5m/s (16.4ft/s). Under this wind condition, the convection coefficient for a concrete deck should be approximately less than 20w/m<sup>2</sup>°C (3.5Btu/hrft<sup>2</sup>°F) (Elbadry and Ghali 1983). Hence, during the temperature model development in the next section, the value of 20w/m<sup>2</sup>°C (3.5Btu/hrft<sup>2</sup>°F) is considered as a good reference to estimate the convection coefficient for GFRP panels.

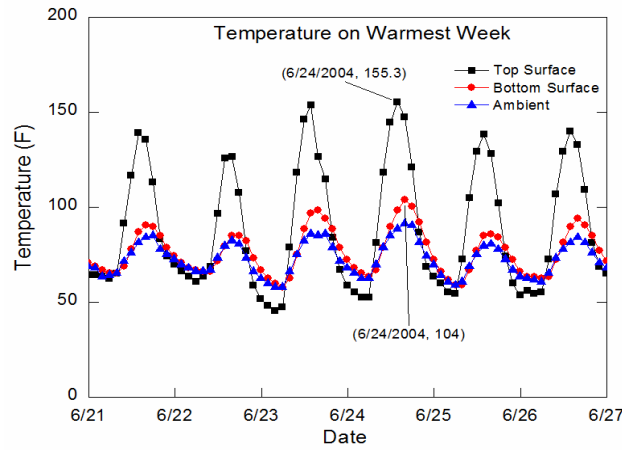


Fig. 3 Measured temperatures from June 21 to June 27, 2004

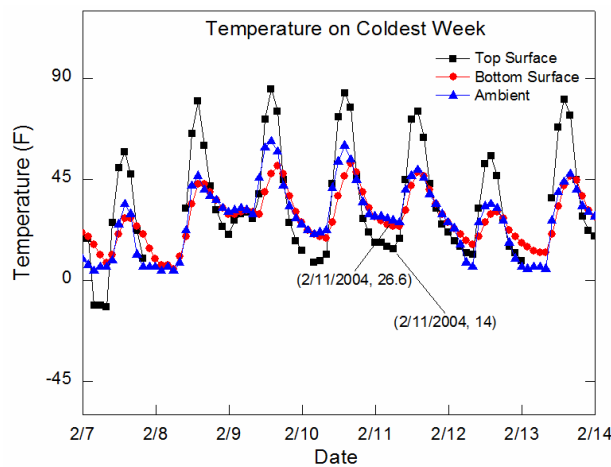


Fig. 4 Measured temperatures from February 7 to February 14, 2004

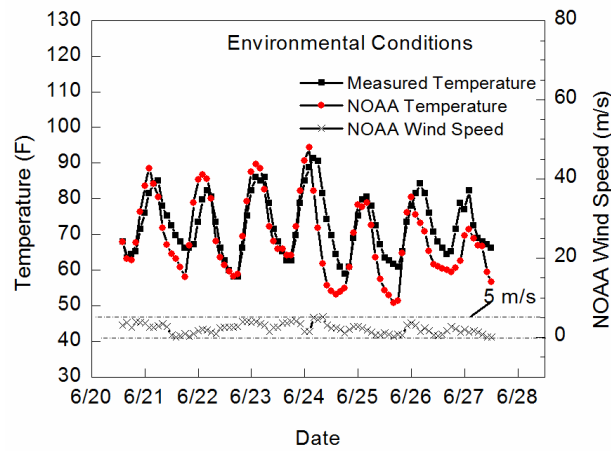


Fig. 5 Environmental conditions from field measurements and weather station

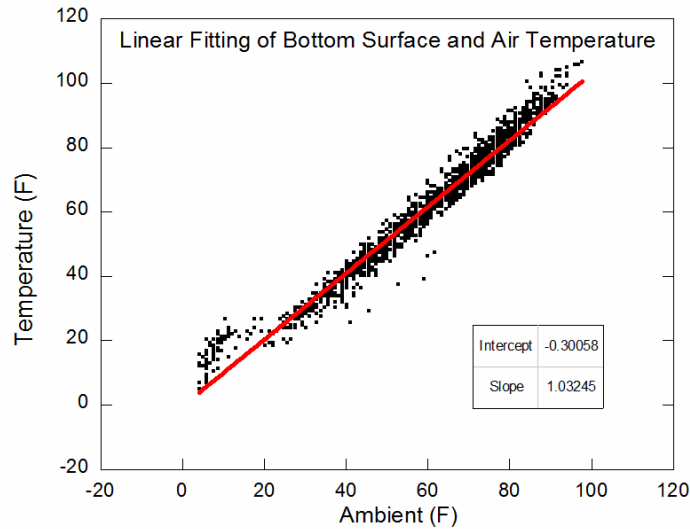


Fig. 6. Fitting of temperatures at the bottom surface of the panel and of the air

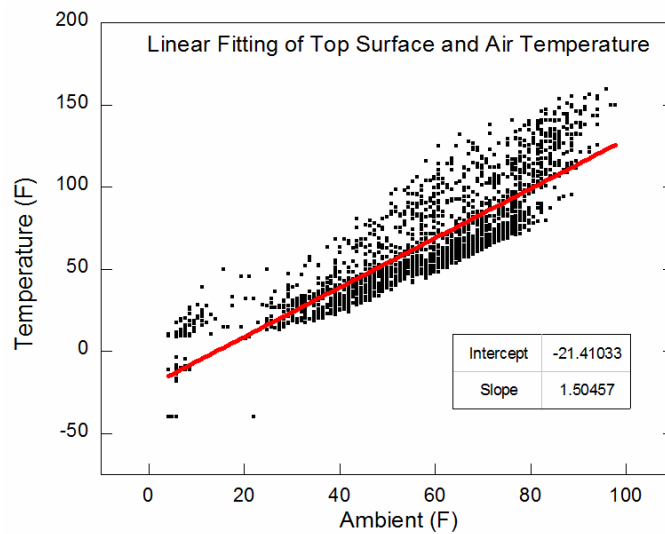


Fig. 7 Fitting of temperatures at the top surface of the panel and of the air

(4) The relationships between the temperatures of the panel surfaces and ambient air are linearly fitted. As is shown in Fig. 6, the bottom surfaces have almost the same temperature as that of the ambient air, while a discrete pattern exists for the relationships between the temperatures at the top surfaces and ambient air, as is shown in Fig. 7. In this sense, for this specific GFRP panel, it is reasonable to use ambient temperatures to represent the temperatures at the bottom surfaces, especially when the measurements are either unavailable or faultily recorded during some periods. For the temperatures at the top surfaces, however, it is not always the case; even though during the night without external solar radiation, the temperatures may tend to approach to that of the ambient air and the linear trends may still be valid.

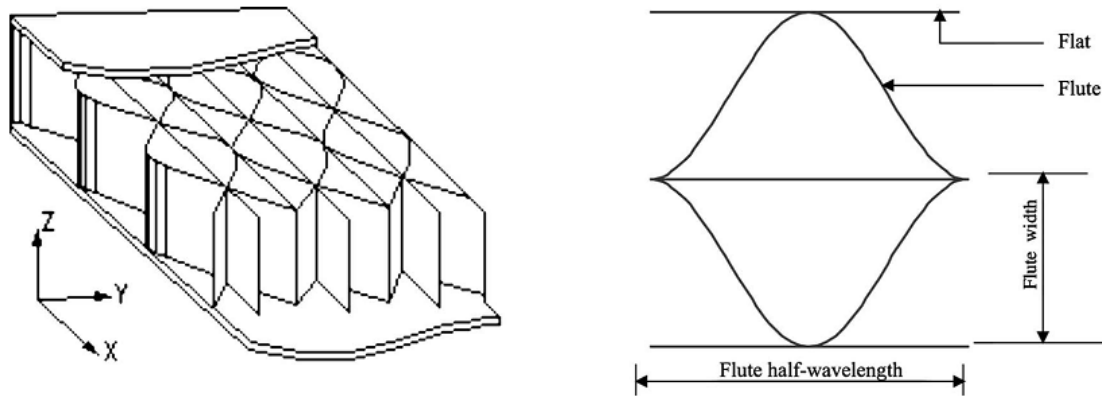


Fig. 8 Sketch of the honeycomb sandwich panel and core configuration

#### 4. Numerical modeling study

The field monitoring observations discussed above provide a qualitative perspective, while several other issues are still unsettled. The temperatures were only recorded at the panel surfaces but not through the slab depths, however, the thermal gradients are often of more importance. For example, the self-equilibrating thermal stress induced from the nonlinear thermal gradients is one of the major reasons causing wearing surface cracks and delamination failures. In addition, the influences of the material thermal properties and environmental parameters are only tentatively explained and correlated with the monitoring results, it is still unclear the effects from each of these parameters on the temperature distributions. Therefore, a numerical modeling approach is proposed and validated in this section. Then, a parametric study is employed to further investigate these uncertainties.

##### 4.1 Prediction of thermal properties

The material properties of the GFRP panels are predicted based on the theory of the micro-macro mechanics method. Basically, the sandwich panel, as is shown in Fig. 8, is made of the E-glass fiber and polyester resin and consists of three parts, i.e., two facial laminates at the top and bottom parts and one core in the middle. The configuration of the sinusoidal core is designed with a flute half-wave length of 10.16 cm (4in) and flute width of 5.08 cm (2in).

The layers, which constitute the facial laminates, include the chopped strand mat (ChSM), continuous strand mat (CSM), bidirectional stitched fabrics, and unidirectional (UNC) layers. Detailed information in terms of the fabrication techniques, geometry descriptions, and constituent layouts of the constituents are referred to Cai *et al.* (2009), Qiao and Wang (2005). From the micro-mechanical perspective of view, the ChSM and CSM layers, made of continuous randomly oriented fibers and having the same properties in all directions, are modeled as the isotropic layers. The UNC layers, with different material properties in the direction parallel and perpendicular to the fibers, are assumed as the orthotropic ones. In this study, the theories and equations adopted for deducing the properties of the GFRP panels are referred to the Composite Materials Handbook (2001) and McCartney and Kelly (2007). Thus, the thermal properties for the laminates of the facial and core are derived and shown in Table 1.

Table 1 Constituents and laminates properties of the GFRP panel\*

Material Units	Density g/cm <sup>3</sup> (lb/in <sup>3</sup> )	Conductivity W/m · K (Btu/hr · ft · °F)	Specific heat J/kg · K (Btu/lb · °F)
E-glass fiber	2.55 (0.092)	1.3 (0.75)	840 (0.2)
Polyester resin	1.14 (0.041)	0.2 (0.12)	1686 (0.4)
Facial laminate	1.59 (0.057)	0.456/0.365/0.333 (0.26/0.21/0.19)	1415 (0.34)
Core Mat	1.47 (0.053)	0.308 (0.18)	1486 (0.36)

\*Note: the densities of the fiber and matrix are given by the manufacture; while the coefficients of the conductivity and specific heat are referred to the online material property database, MATWEB (<http://www.matweb.com/>), and the literature (Bai *et al.* 2008).

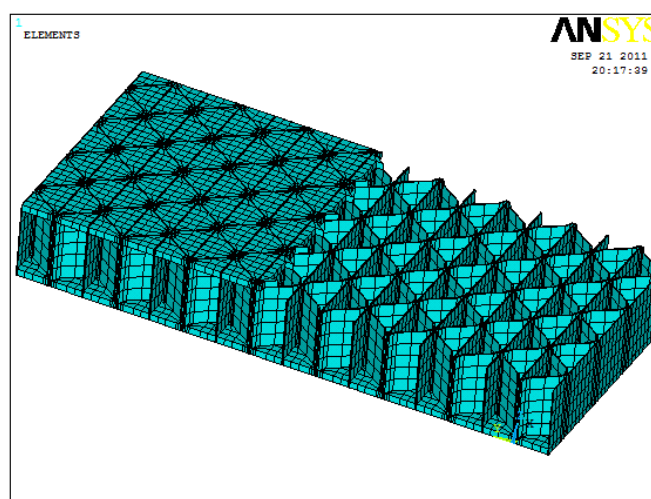


Fig. 9 Finite element model of the GFRP panel

#### 4.2 Numerical modeling method

The heat transfer mechanisms introduced in the previous section are simulated using the commercial software ANSYS 11.0, as the model shown in Fig. 9. Since the boundary conditions and temperature distributions are all time-varying, a transient-state thermal field analysis is conducted for the GFRP panels. The heat transfer behaviors within the hollow section from the entrapped air and inner surfaces' mutual radiation are neglected at this stage and their effects are discussed in the next parametric study section. Therefore, the temperature variations of the panels are numerically simulated for the warmest week from 02:00 on 6/21/2004 to 24:00 on 6/27/2004 with a two-hour interval. The ambient air temperature is directly obtained from the field measurements, and the solar flux is calculated based on the methodology introduced above. The initial bridge temperature is assumed as the average value of the maximum and minimum air temperatures. The errors induced from this assumption is offset by continuously running the programs three cycling periods, i.e., 72 hours with 24-hour each, under the same environmental conditions, as discussed by Dilger *et al.* (1983). All the parameters used in the finite element model are shown in Table 2.

Table 2 Parameters used in the FEM of the GFRP panel

Date	6.21 to 6.27, 2004
Time	02:00 to 24:00
Location	Crawford County, KS, 38° N /95°W
Air Pressure	0.968
Environmental Turbidity	1.8
Top/Bot. Surface Convection	15 W/m <sup>2</sup> °C (2.64 Btu/hrft <sup>2</sup> °F)
Top/Bot. Surface Solar Emissivity	0.5/0.3
Top/Bot. Solar Absorptivity	0.8

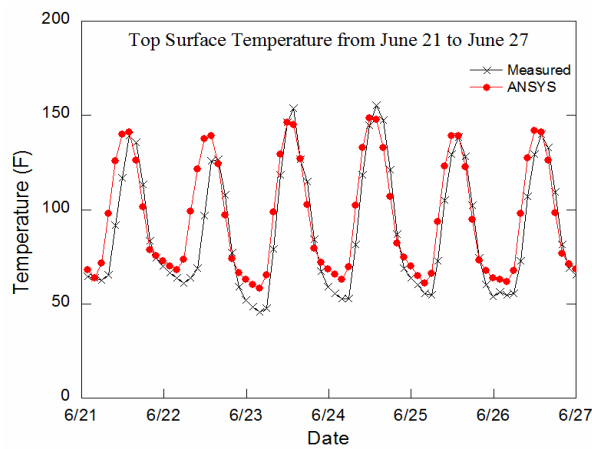


Fig. 10 Temperature comparisons at the top surfaces of the GFRP panel

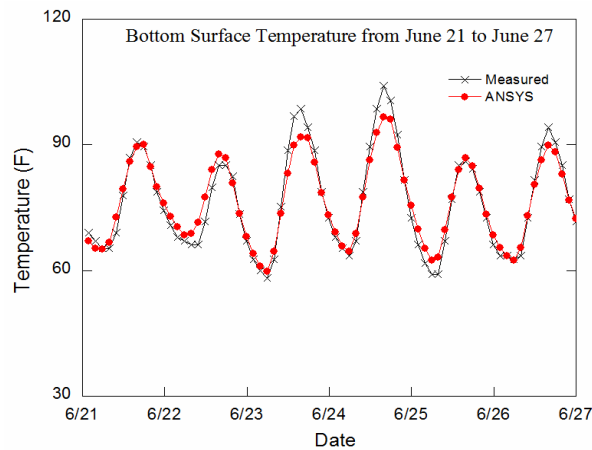


Fig. 11 Temperature comparisons at the bottom surfaces of the GFRP panels

#### 4.3 Comparison of results

The predicted temperatures at the top and bottom surfaces from June 21 to June 27 in 2004 are plotted in Fig. 10 and Fig. 11, respectively. It can be observed through comparisons that the results

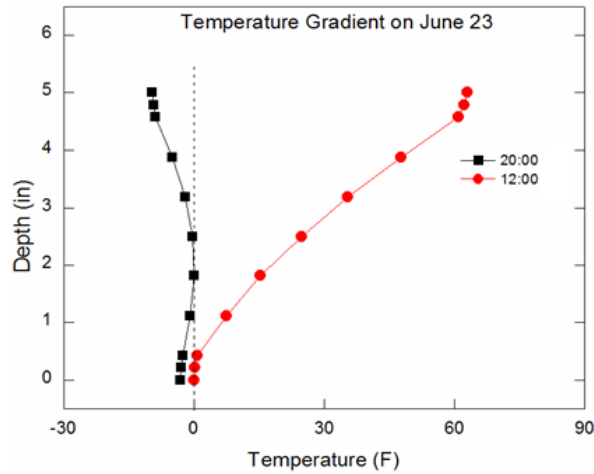


Fig. 12 Predicted positive and negative thermal gradients on June 23, 2004

from the measurements and predications match well with each other. Thus, the modeling methodology together with the corresponding thermal properties and environmental parameters is valid. Fig. 12 shows the predicted maximum positive and negative gradients appearing at 12:00 and 20:00 on June 23, respectively, where the plotted data is normalized by subtracting the minimum temperature values along the panel depths. It can be observed that the nonlinear distribution patterns appear along the depth of the current GFRP panels, even though the nonlinearity is not significantly evident due to the shallow depth of the GFRP panels.

## 5. Parametric study

With the proposed modeling approach, the effects of several temperature influencing factors are further investigated in a parametric study, including the section hollowness, environmental conditions, and material thermal properties. All the parameters that were adopted in the previous model development stage are used here again. The corresponding results without considering the section hollowness effects are taken as the base case throughout the following discussions. Since the 12.7cm (5in) GFRP panel adopted in this project does not show significant nonlinear thermal gradients, as indicated in Figure 12, a more popular and deeper 25.4cm (10in) GFRP panel with the same material properties is selected and analyzed in this parametric analysis. Therefore, the maximum positive and negative thermal gradients occurring at 12:00 and 22:00 on June 23, 2004, respectively, are simulated and discussed. The thermal gradients are plotted both for the absolute and normalized values, where the normalized results refer to the ones after subtracting the minimum temperatures from the absolute values along the panel depths, i.e., by setting the minimum value as zero.

### 5.1 Air convection

During the daytime, the top surface of the panel is heated by the solar radiation. Then, the high energy further conducts through the panel depth and heats both the structure elements and ambient

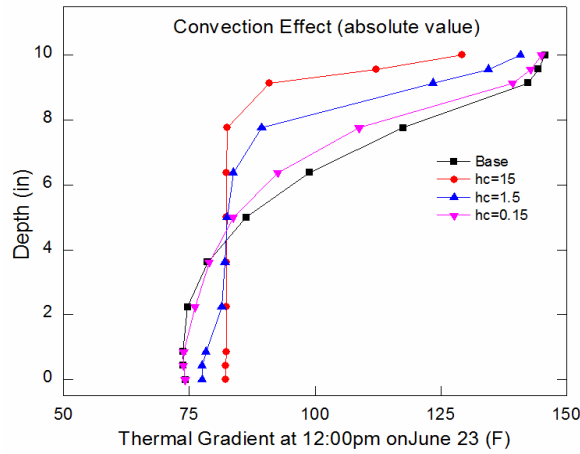


Fig. 13 Absolute thermal gradients under convection effects at 12:00, June 23

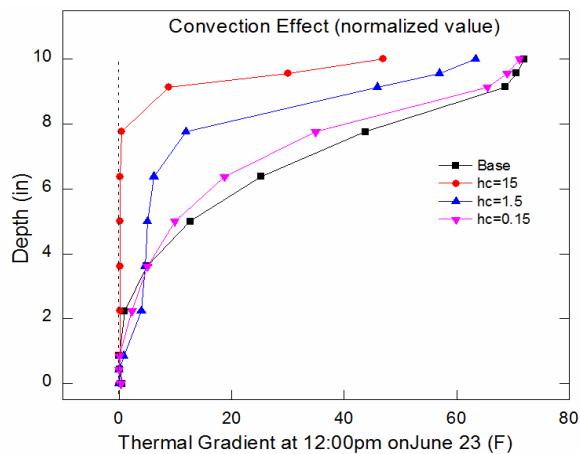


Fig. 14 Normalized thermal gradients under convection effects at 12:00, June 23

air inside the hollow section. During the night, however, with the external heat decreasing and surface cooling, the energy is reversely transferred from the inner to the outer sides of the panels. Through this procedure, the induced temperature differences within the hollow section, between the inner ambient air and the surrounding structural surfaces, develop an additional thermal convection system. Hence, the effects of this mechanism on the temperature distributions are simulated by varying the thermal convection coefficients ( $h_c$ ) between the inner surfaces and inner ambient air, where the inner air temperatures are assumed to be the same as that of the ambient air.

Fig. 13 shows the absolute temperature distributions due to the entrapped air convection effects during the daytime with different  $h_c$ . The inner convection behavior is observed to have more evident effects on the temperatures generated at the top parts of the panels than that at the bottom. For example, with the increase of the convection behaviors, the temperature values tend to decrease more at the top parts but increase less at the bottom. In addition, Fig. 14 shows the normalized thermal gradients from the effects of the inner convection behavior. As is observed, with the increase of  $h_c$ , the nonlinear thermal gradients are obviously more linear for the locations

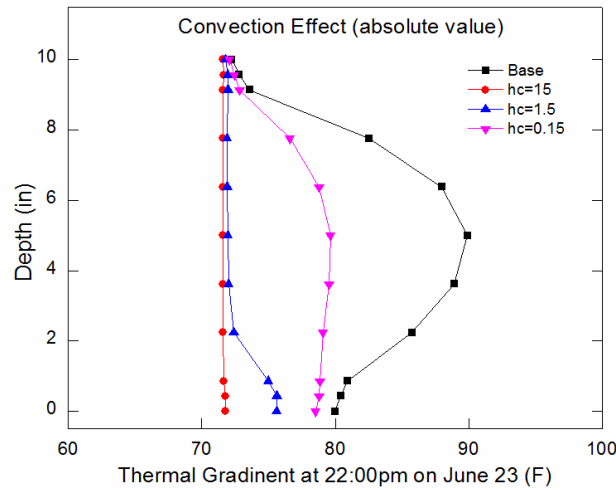


Fig. 15 Absolute thermal gradients under convection effects at 22:00, June 23

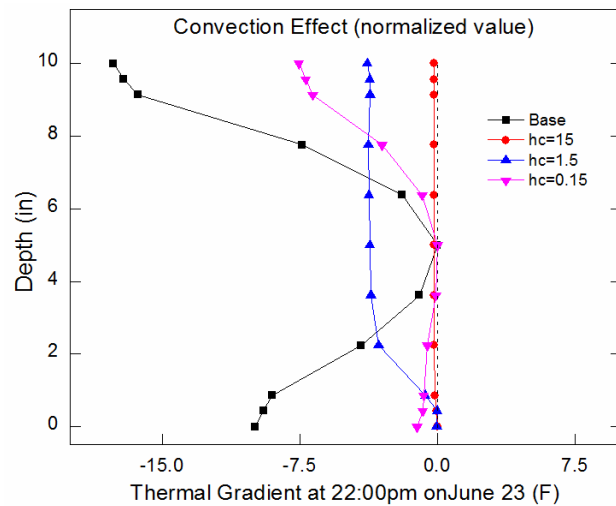


Fig. 16 Normalized thermal gradients under convection effects at 22:00, June 23

away from the top surfaces towards the panel depths; while the temperatures at the top surfaces are still largely varied by the solar radiation.

Similar phenomenon can be observed for negative thermal gradients during the night. As is shown in Fig. 15, when the temperatures at top surfaces are consistent with that of the ambient air, the convection behavior almost disappears, and the high temperature at bottom surfaces tends to approach to that of the ambient air with the increase of convection behaviors. Thus, the final maximum and minimum negative thermal gradients, as is shown in Fig. 16, appear at the conditions with the smallest and largest  $h_c$  values, respectively. Therefore, it can be concluded that the inner air convection behavior tends to reduce the nonlinear gradient patterns and to make the temperatures more uniformly distributed. Thus, if ignoring the inner air convection behaviors in the numerical modeling, the induced thermal gradients are much larger.

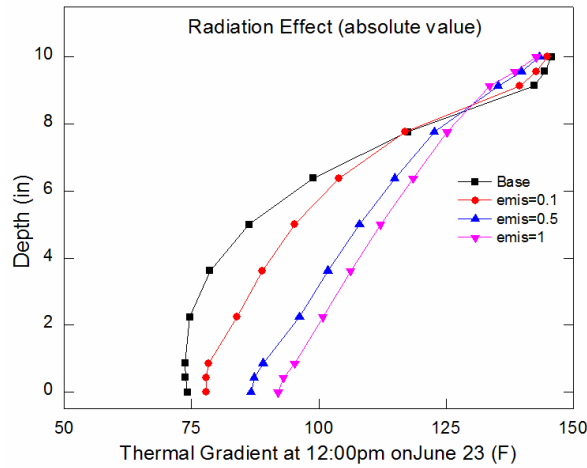


Fig. 17 Absolute thermal gradients under radiation effects at 12:00, June 23

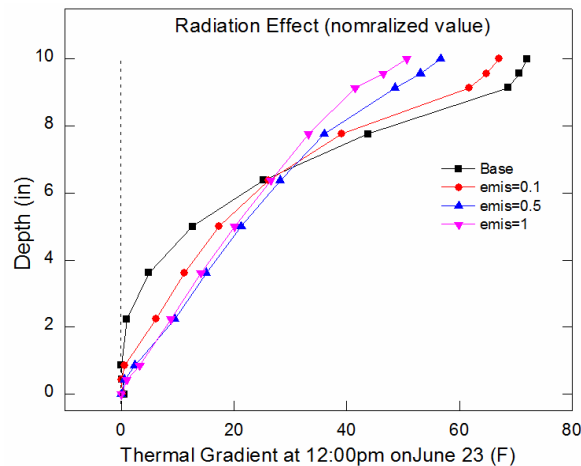


Fig. 18 Normalized thermal gradients under radiation effects at 12:00, June 23

### 5.2 Mutual radiation

Besides the convection behaviors, the temperature differences among the surrounding structure surfaces within the hollow section can generate an additional mutual radiation heat transfer mechanism. The effects of this behavior on the temperature gradients are simulated using the AUX12 Radiation Matrix Method provided in ANSYS 11.0. Specifically, the form factors are defined to account for the relative positions between two mutual radiating surfaces. The material surface emissivity properties, referring to the ratio of the radiation emitted by a face to that emitted by a black body under the same temperature, are varying in the models. Fig. 17 shows the absolute temperature gradients due to the inner surface mutual radiation at 12:00. With the increase of the emissivity coefficients, labeled as “emis” in the figure, the temperatures at the top surfaces are negligibly affected, while the temperatures at bottom surfaces are apparently increased. Again, the nonlinear temperature distribution trends, as is shown in Fig. 18, tend to be smoothed out, and the

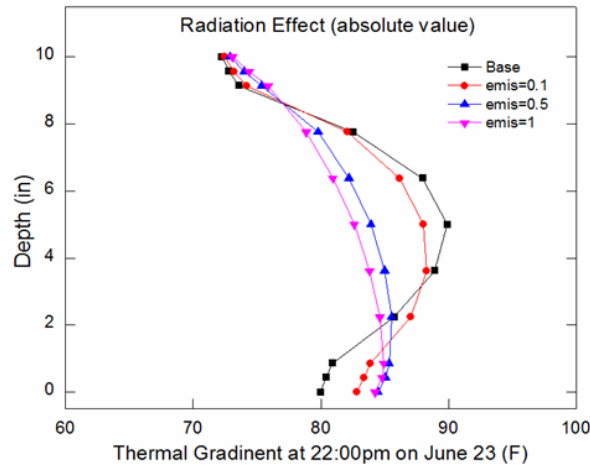


Fig. 19 Absolute thermal gradients under radiation effects at 22:00, June 23

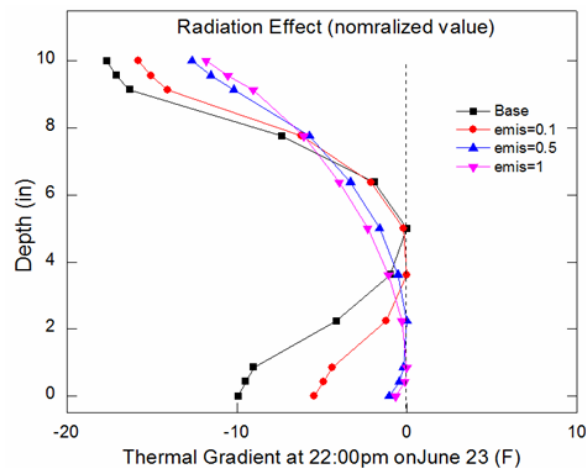


Fig. 20 Normalized thermal gradients under radiation effects at 22:00, June 23

highest mutual radiation coefficient leads to almost a linear temperature gradient. During the night, with the increase of the emissivity, the absolute temperatures at the surfaces varies less, as is shown in Fig. 19; but the nonlinear temperature gradients are significantly softened, as is shown in Fig. 20. Therefore, it can be concluded that with the considerations of the inner surface mutual radiation, the nonlinear thermal gradients tend to be more linear.

### 5.3 Environmental and material properties

The effects of the material properties and environmental parameters on the thermal gradients of GFRP panels are discussed by comparing the predicted temperatures after artificially increasing and decreasing all the parameters by 25%. The corresponding temperature changes, at the top surfaces, middle sections, bottom surfaces, and the differences between the maximum and minimum temperatures through the panel depths at 12:00 on June 23, 2004 are listed in Table 3.

Table 3 Predicted temperatures at 12:00, June 23, from the parametric study

Parameters	Top Surface		Middle Section		Bottom Surface		Difference	
	Inc.	Dec.	Inc.	Dec.	Inc.	Dec.	Inc.	Dec.
Environmental Turbidity	-1.94%	2.03%	-1.14%	1.22%	-0.07%	0.07%	-3.46%	3.60%
Solar absorption	10.53%	-10.65%	5.01%	-5.05%	0.23%	-0.23%	19.33%	-19.55%
Maximum temperature	12.25%	-12.26%	8.89%	-8.80%	18.73%	-18.15%	11.63%	-9.44%
Minimum temperature	1.30%	-1.30%	7.59%	-7.56%	5.65%	-5.70%	-5.32%	5.32%
Conductivity	-0.06%	0.05%	5.15%	-6.24%	0.35%	-0.11%	-3.24%	3.58%
Specific heat	-0.31%	0.28%	-5.47%	7.84%	-2.22%	3.05%	3.35%	-5.46%
Density	-0.30%	0.27%	-5.62%	7.29%	-2.18%	2.90%	3.41%	-5.09%
Top surface convection	-7.80%	10.22%	-3.52%	4.58%	-0.16%	0.21%	-14.38%	18.85%
Bot. surface convection	0.00%	0.00%	0.11%	-0.11%	0.94%	-1.07%	-0.55%	0.60%
Top surface emissivity	-1.30%	1.39%	-0.54%	0.57%	-0.02%	0.02%	-2.42%	2.60%
Bot. surface emissivity	0.00%	0.00%	0.16%	-0.16%	1.27%	-1.50%	-0.74%	0.83%

Some of the important findings are discussed as follows:

Firstly, the temperatures at the panel surfaces are literally affected by the environmental conditions and material surface properties. For example, the coefficients of the solar absorptivity and the top surface thermal convection show the determining effects on the temperatures at the top surfaces, where a large coefficient leads to significant temperature differences along the panel depths. Secondly, the change of the daily extreme temperatures affects the total temperature fields, and that in turn influences the temperatures of the bridge components. For example the increase of the daily maximum temperatures increases the temperatures at the top surfaces and also the temperature gradients through the depths. Thirdly, the material properties, such as the thermal conductivity, specific heat, and density, have negligible effects on the temperatures generated at the surfaces but affect the thermal conduction abilities to some degree, even though these effects are not as considerably important as that of the environmental conditions. Finally, for all the other parameters, their influences on the GFRP panel temperature distribution behaviors are insignificant and can be ignored.

## 6. Conclusions

The temperature field of GFRP honeycomb hollow section sandwich panels is investigated in this paper. Based on the field monitoring program conducted by the Kansas DOT, the temperature distribution patterns at the top and bottom surfaces of the panels are demonstrated and discussed. The proposed thermal field modeling methodology, together with the predicted thermal properties and environmental parameters, is verified through comparing the simulated results with that of the field measurements. The effects of the hollow section configurations, thermal properties, and environmental conditions are investigated through a parametric analysis. Based on the present study, it can be concluded as follows:

(1) Significant temperature differences can be induced between the top and bottom surfaces of the GFRP panels; and that is attributed to the hollow section configurations and the low thermal conductivities of GFRP materials. The temperatures at the top surfaces are highly related to the

hourly-varying solar radiation; while the temperatures at the bottom surfaces tend to approach to that of the ambient air due to the air convection.

(2) The available temperature design criteria in the AASHTO LRFD (2007) for traditional concrete slabs is no longer valid for GFRP panels since the measured temperatures have exceeded the range stipulated in the code. Since the monitoring results may not completely cover all the worst conditions, it may be implied that the critical thermal gradients for the GFRP panels may be much larger, and the negative temperature gradients are more important.

(3) The thermal gradients for the 12.7cm (5in) GFRP panel utilized in the project, though not very evident yet, tends to be nonlinearly distributed. With the increase of the slab depth, the nonlinear temperature distribution patterns become more apparent. It should be noted that the temperature distribution discussed in this study only refers to the panel itself. A different behavior should be expected if assembling the FRP panels on the concrete beams or steel girders.

(4) The heat transfer mechanisms within the hollow section, from the inner air convection and mutual surfaces radiation, produce smaller effects on the temperatures generated at the panel surfaces, but make significant influences on the thermal gradients through the panel depths. In addition, a neglect of these heat transfer behaviors during the numerical studies often produces more nonlinear temperature differences.

(5) The environmental parameters, i.e., daily maximum temperature, solar radiation (expressed by the material surface absorptivity coefficient), and the wind speed (expressed by the material surface convection coefficient), are the primary factors determining the temperature distribution behaviors of GFRP panels; while the material thermal properties only influence the thermal gradients to a small extent.

## Reference

- AASHTO LRFD Bridge Design Specifications 4th Edition (2007), Washington, DC, U.S.A.
- ANSYS (2012), ANSYS theory reference, 11.0, ANSYS, Inc.
- Bai, Y., Vallee, T. and Keller, T. (2008), "Modeling of thermal responses for FRP composites under elevated and high temperatures", *Composites Science and Technology*, **68**(1), 47-56.
- Bakis, C.E., Bank, L.C., Brown, V.L., Cosenza, E., Davalos, J.F., Lesko, J.J., Machida, A., Rizkalla, S.H., and Triantafillou, T.C. (2002), "Fiber-reinforced polymer composites for construction-state-of-the-art review", *Journal of Composites for Construction*, **6**(2), 73-87.
- Cai, C.S., Oghumu, S.O. and Meggers, D.A. (2009), "Finite-element modeling and development of equivalent properties for FRP bridge panels", *Journal of Bridge Engineering*, **14**(2), 112-121.
- Composite Materials Handbook-MIL 17, Volume III: Materials Usage, Design, and Analysis (2001), Department of Defense Handbook.
- Dilger, W.H., Ghali, A., Chan, M., Cheung, M.S. and Maes, M.A. (1983), "Temperature stresses in composite box girder bridges", *Journal of Structural Engineering*, **109**(6), 1460-1478.
- Duffie, J.A. and Beckman, W.A. (1980), *Solar engineering of thermal processes*, John Wiley and Sons, New York.
- Elbadry, M.M. and Ghali, A. (1983), "Temperature variations in concrete bridges", *Journal of Structural Engineering*, **109**(10), 2355-2374.
- Foster, D.C., Richards, D. and Bogner, B.R. (2000), "Design and installation of fiber-reinforced polymer composite bridge", *Journal of Composites for Construction*, **4**(1), 33-37.
- Hollaway, L.C. (2010), "A review of the present and future utilization of FRP composites in the civil infrastructure with reference to their important in-service properties", *Construction and Building Materials*, **24**(12), 2419-2445.

- Laosiriphong, K., GangaRao, H.V.S., Prachasaree, W. and Shekar, V. (2006), "Theoretical and experimental analysis of GFRP bridge deck under temperature gradient" *Journal of Bridge Engineering*, 11(4), 507-512.
- Liu, W.J., Zhou, E., Wang, Y.Q., Meggers, D.A. and Plunkett, J. (2008), "Long-term remote monitoring of thermal response of No-Name Creek FRP bridge to climate", *Transportation Research Board 87<sup>th</sup> Annual Meeting Conference*, No. #08-1137
- McCartney, L.N. and Kelly, A. (2007), "Effective thermal and elastic properties of [+ $\theta$ /- $\theta$ ]s laminates", *Composites Science and Technology*, 67(3-4), 646-661.
- Meggers, D.A. (2006), *Personal communication*, Kansas Department of Transportation.
- Mirambell, E. and Aguado, A. (1990), "Temperature and stress distributions in concrete box girder bridges", *Journal of Structural Engineering*, 116(9), 2388-2409.
- Moorty, S. and Roeder, C.W. (1992), "Temperature-dependent bridge movements", *Journal of Structural Engineering*, 118(4), 1090-1105.
- Oghumu, S.O. (2005), "Finite element modeling approach and performance evaluation of fiber reinforced polymer sandwich bridge panels", Master Thesis, Department of Civil and Environmental Engineering, Louisiana State University.
- Priestley, M. J. N. (1978), "Design of concrete bridges for temperature gradients", *ACI Journal*, 75(5), 209-217.
- Qiao, P.Z. and Wang, J.L. (2005), "Mechanics of composite sinusoidal honeycomb cores", *Journal of Aerospace Engineering*, 18(1), 42-50.
- Reising, R.M.W., Shahrooz, B.M., Hunt, V.J., Neumann, A.R. and Helmicki, A.J. (2004), "Performance comparison of four fiber-reinforced polymer deck panels", *Journal of Composites for construction*, 8(3), 265-274.
- Tipirneni, R.R. (2008), "Characterization of thermal and electrical properties of fiber reinforced polymer (FRP) composite", Master Thesis, College of Engineering and Mineral Resources, West Virginia University.